

On the total cosmological information in galaxy clustering: an analytical approach

M. Wolk^{*}, J. Carron and I. Szapudi

Institute for Astronomy, University of Hawaii, 2680 Woodlawn Drive, Honolulu, HI, 96822

29 October 2021

ABSTRACT

Beyond the linear regime of structure formation, part of cosmological information encoded in galaxy clustering becomes inaccessible to the usual power spectrum. *Sufficient statistics*, A^* , were introduced recently to recapture the lost, and ultimately extract all, cosmological information. We present analytical approximations for the A^* and traditional power spectra as well as for their covariance matrices in order to calculate analytically their cosmological information content in the context of Fisher information theory. Our approach allows the precise quantitative comparison of the techniques with each other and to the total information in the data, and provides insights into sufficient statistics. In particular, we find that while the A^* power spectrum has a similar shape to the usual galaxy power spectrum, its amplitude is strongly modulated by small scale statistics. This effect is mostly responsible for the ability of the A^* power spectrum to recapture the information lost for the usual power spectrum. We use our framework to forecast the best achievable cosmological constraints for projected surveys as a function of their galaxy density, and compare the information content of the two power spectra. We find that sufficient statistics extract all cosmological information, resulting in an approximately factor of $\simeq 2$ gain for dense projected surveys at low redshift. This increase in the effective volume of projected surveys is consistent with previous numerical calculations.

Key words: cosmology: large-scale-structure of the Universe, methods : analytical, methods, cosmology : cosmological parameters

1 INTRODUCTION

Within the current inflationary paradigm of cosmology, the small initial density fluctuations are believed to be very close to Gaussian statistics. The most natural observables of such a field, the two-point statistics, lose some of their statistical power as non-linear gravitational growth induces correlations between Fourier modes (Rimes & Hamilton 2005; Neyrinck et al. 2006). These correlations, especially those between large and small scales, diminish the amount of information accessible to these two-point statistics. A fraction of this hidden information is accessible to higher-order N -point statistics (e.g., Peebles 1980; Szapudi 2009). They are, however, not only difficult to measure and interpret due to a combinatorial explosion of complexity, but they fail to capture all available cosmological information, increasingly so on more non-linear scales. (Carron & Neyrinck 2012; Carron & Szapudi 2013, and references therein).

Non-linear transformations, such as the logarithmic mapping (Neyrinck et al. 2009) or variants thereof (Seo

et al. 2011; Joachimi & Taylor 2011) were introduced specifically to retrieve the total information content of the matter field. Carron & Szapudi (2013) defined *sufficient statistics* as an observable extracting all cosmological information from data. They have demonstrated in the context of perturbation theory and N -body simulations that the logarithmic transformation, $A = \ln(1 + \delta)$, approximates well the exact sufficient statistics of the dark matter field. Note that in the case of a continuous lognormal field A is the exact sufficient statistics, a statement supported by analytical calculations and measurements in simulations (Carron et al. 2014a, and references therein).

In a previous work, Carron & Szapudi (2014) introduced the local non-linear transformation A^* as the optimal observable to extract the information content of galaxy count maps. This recaptures in its spectrum the total available cosmological information in presence of shot-noise. The new observable has been characterized in detail using numerical simulations of 2-dimensional survey configurations (Wolk et al. 2014; Carron et al. 2014a). Yet, the precise manner in which A^* recaptures the cosmological information remained somewhat of a puzzle, given that its shape closely resem-

^{*} E-mail: wolk@ifa.hawaii.edu

bles that of the power spectrum. In this work, we present an analytical theory of the total information content (i.e. the constraining power) of the A^* angular power spectrum for cosmological parameters, assuming that we have access to the power spectrum and its derivatives as a function of cosmological parameters; this is provided by a standard Boltzmann code, such as CAMB (Lewis et al. 2000). Our approach is then used to compare sufficient statistics with the usual angular galaxy power spectrum as a function of the relevant projected survey characteristics, most importantly the shot noise level. The analytical approach provides insight into the workings of sufficient statistics, in particular it sheds light on the crucial role played by the bias of the non-linear transformation in recapturing the lost information.

To test its validity, we carefully compare our model to the predictions from our previous numerical simulations. For simplicity of expression, we will designate these numerical results as “exact” throughout this work. In practice, these simulations provide accurate enough results that this nomenclature is justified. Throughout this paper, the notation $P(k)$ is used to designate the angular power spectrum with $k \simeq \ell + 1/2$ in the flat sky approximation.

Section 2 describes the analytical ansatz for the A^* bias and covariance matrix. Described in Section 3 is the model for the 2-dimensional matter field covariance matrix. With this model, we estimate the information content for different survey densities as presented in Section 4. Our estimations are also compared to previous numerical predictions of Wolk et al. (2014). We summarize and conclude with a discussion in Section 5.

2 ANSATZ FOR THE A^* BIAS AND COVARIANCE MATRIX

Assuming that the galaxy counts Poisson sample an underlying lognormal galaxy field, let $N = (N_1, \dots, N_{n_{\text{cells}}})$ be a map of galaxy counts. In the following, $n_{\text{cells}} = 128^2$, for a two dimensional map. Given a sampling rate \bar{N} , the mapping from N to A^* is defined by the non-linear equation (Carron & Szapudi 2014):

$$A^* + \bar{N} \sigma_*^2 e^{A^*} = \sigma_*^2 \left(N - \frac{1}{2} \right), \quad (1)$$

where $\sigma_*^2 = \ln(1 + \sigma_{\delta_g}^2)$, with $\sigma_{\delta_g}^2$ the variance of the galaxy field fluctuations at the cell scale. These A^* -mapping parameters are estimated using our fiducial cosmology and are then kept fixed. Given the current precision of cosmological parameters this assumption amounts to no practical limitations for our technique.

Wolk et al. (2014), using a simulation pipeline calibrated on the Canada-France-Hawaii Telescope Legacy Survey (CFHTLS)¹ data, have shown that the information gain using the mean and spectrum of A^* instead of the galaxy power spectrum on the three cosmological parameters Ω_m , σ_8 and w_0 is up to about a factor of 2, especially at low redshifts and for dense surveys. This numerical approach clearly demonstrated that the “sufficient statistics” A^* performs better, yet, it could not yield qualitative insights into

workings of sufficient statistics. Given that the shape of the A^* power spectrum is very similar to the usual power spectrum the question naturally arises: is the increase of information attributed to A^* itself, more precisely its derivatives being more sensitive to parameters, or, to the fact that the corresponding covariance matrix is better behaved, in particular more diagonal? In our analytical approach next we point out the crucial cosmological dependence of the bias, and show that part of the information gain in fact can be pinned on the derivatives of the bias with respect to cosmological parameters.

2.1 From the galaxy power spectrum to the A^* -power spectrum

Our analytical approach assumes prior knowledge on the galaxy power spectrum $P_{\delta_g} \equiv P$ as function of cosmological (and halo) parameters. We use the standard, unweighted power spectrum estimator:

$$\hat{P}(k) = \frac{1}{VN_k} \sum_{k'} |\delta(k')|^2 \quad (2)$$

with V the survey volume and where the sum runs over the N_k Fourier modes associated to the k -th power spectrum bin. This simple estimator is optimal for simple geometries, such as N -body simulations. Including complications from survey geometry and the corresponding optimal weighting of the estimator will not change any of our results, as the scales we are focussing on are small enough that edge effects will become unimportant. We model the galaxy clustering with the Halo Occupation Distribution (HOD) description of Wolk et al. (2014) and the CosmoPMC² package. We consider four different redshift bins: $0.2 < z < 0.4$, $0.4 < z < 0.6$, $0.6 < z < 0.8$ and $0.8 < z < 1.0$. Figure 1 shows the A^* - and galaxy power spectra for the redshift bin $0.6 < z < 0.8$ with their 1σ confidence regions (shaded) as well as the predictions of the power spectra for the underlying fields δ_g and $A = \ln(1 + \delta_g)$ (blue dotted lines).

The first step is to model the bias between the spectra of the two continuous fields δ_g and $A = \ln(1 + \delta_g)$. Here we assume a lognormal underlying galaxy density, an hypothesis that have been proved to be very accurate in 2D (Carron et al. 2014a). Then the simplest Ansatz to consider is the ratio of the variances, and for the lognormal model the variances are related as $\sigma_A^2 = \ln(1 + \sigma_{\delta_g}^2)$. Explicitly, we assume

$$P_A = b_A^2 P \quad (3)$$

where:

$$b_A^2 = \frac{\sigma_A^2}{e^{\sigma_A^2} - 1}. \quad (4)$$

According to the left panel of Figure 3, this approximation is better than 4% accurate on all the k -range, even if it starts to deviate slightly both for very large or very small scales. This formula, in the regime of low A -variance, reduces to that of Neyrinck et al. (2009) $b_A^2 = e^{-\sigma_A^2}$ obtained from simulations for the 3-dimensional power spectrum.

¹ <http://www.cfht.hawaii.edu/Science/CFHTLS/T0007/>

² <http://cosmopmc.info>

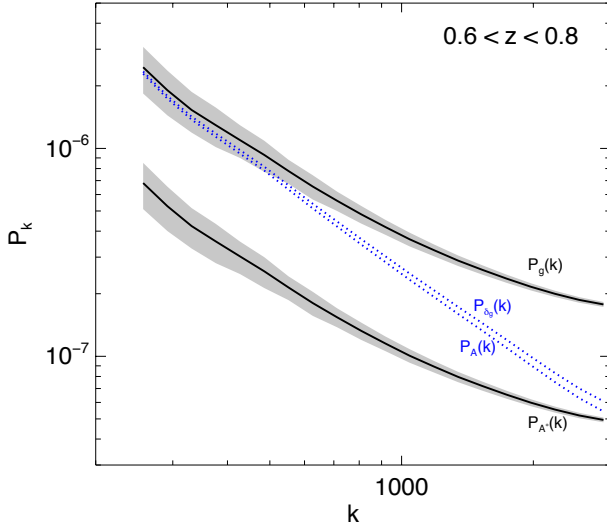


Figure 1. Predictions of both the galaxy angular power spectrum $P_g(k)$ and the non-linear transform A^* power spectrum $P_{A^*}(k)$ in the redshift bin $0.6 < z < 0.8$. The grey area show the 1σ confidence regions. The blue dotted lines represent the power spectra of the underlying fields δ_g and $A = \ln(1 + \delta)$ and thus illustrate the effect of shot-noise.

2.2 From continuous to discrete fields

The link between the continuous and discrete galaxy field power spectra is well understood for Poisson sampling through $P_g = P + 1/\bar{n}$ where \bar{n} is the density of the considered survey related to the sampling rate via $\bar{n} = \bar{N}n_{\text{cells}}/V$. V is the survey volume and is fixed here to the size of the CFHTLS-W1 field $L = 7.46$ degrees on the side. As it will be explained in more details in Section 3, considering the local lognormal case will result in a cancellation of the contribution from the super survey modes in the galaxy power spectrum covariance matrix, hence implying that the information content does not depend on the survey geometry. Then, how could the relationship be explained between the A - and the A^* power spectra?

From Equation 1, it can be expected that this relationship depends on the A^* -mapping parameters and especially on \bar{N} as, at a particular redshift and n_{cells} , σ_* is fixed. Figure 2 shows the scatter plot of A^* as a function of A for two different values of \bar{N} , the first one corresponding to the sampling rate of the CFHTLS-W1 field in the redshift bin $0.6 < z < 0.8$.

When the survey is dense, i.e. when \bar{N} is large enough, there is almost no bias between A and A^* meaning that the local transformation A^* traces well the underlying field. In contrast, for a low density survey, A^* tends to be smaller than A leading to less fluctuations thus less power in A^* in agreement with the simulations on Figure 1. Hence most of the bias is due to the fact that, for low \bar{N} , A^* cannot distinguish between low A regions or a cell that happens to be empty due to a low \bar{N} (a non-local generalization of A^* would potentially behave better Carron & Szapudi 2013).

The next step is to relate the galaxy power spectrum to the A^* power spectrum. In order to take the shot-noise

contribution into account, we develop to the 2nd order expansion around zero for the exponential term of Equation 1 and then take the Fourier transform:

$$\left[\frac{1}{\sigma_*^2} + \bar{N}e^{A^*} \right]^2 P_{A^*} = P_N = \bar{N}^2 P_g = \bar{N}^2 \left[P + \frac{1}{\bar{n}} \right]. \quad (5)$$

Thus the bias has a simple form:

$$P_{A^*} = \frac{b_{A^*}^2}{b_{A^*}^2} P_g = \frac{b_{A^*}^2}{b_{A^*}^2} \left[P + \frac{1}{\bar{n}} \right] \quad (6)$$

where

$$b_{A^*}^2 = \left(1 + \frac{1}{\bar{N}\sigma_*^2} \right)^2 \quad (7)$$

The right panel of Figure 3 shows the A^* - and galaxy power spectra as well as the prediction from Equation 6. The accuracy is better than 0.5% over the whole k -range.

2.3 The A^* covariance matrix

To quantify its Fisher information content, we need an estimation of the A^* -covariance matrix:

$$\text{Cov}_{ij}^{A^*} = \langle \hat{P}_{A^*}(k_i) \hat{P}_{A^*}(k_j) \rangle - \langle \hat{P}_{A^*}(k_i) \rangle \langle \hat{P}_{A^*}(k_j) \rangle \quad (8)$$

We found previously that a diagonal Gaussian covariance provides an accurate model:

$$\text{Cov}_{ij}^{A^*} = \frac{2}{N_k} P_{A^*}(k_i) P_{A^*}(k_j) \delta_{ij}, \quad (9)$$

where the A^* -power spectrum is given by Equation 6. This is further motivated by the fact that i) Carron & Szapudi (2013) have shown non-linear transformations tend to Gaussianize the field, ii) in our model of lognormal underlying distribution, it would be exact in the absence of shot-noise (i.e. when \bar{N} goes to infinity) and iii) taking shot-noise into account tends to increase the diagonal part of the covariance matrix adding an extra term $(1/\bar{n})^2$.

The left panel of Figure 4 shows the diagonal of the matrix obtained using Equation 9 as a function of the exact value. The agreement is almost perfect on the diagonal between the two quantities. The middle panel represents the comparison between the approximate (lower right) and the exact (upper left) values of the normalised A^* -covariance matrix. The analytical formula reproduces the exact prediction at the 10% level or better. To quantify the impact of these discrepancies on the non-diagonal terms, we can consider the squared cumulative signal-to-noise for A^* defined as:

$$(S/N)^2 = \sum_{k_i, k_j \leq k_{\text{max}}} P_{A^*}(k_i) [\text{Cov}_{ij}^{A^*}]^{-1} P_{A^*}(k_j) \quad (10)$$

as a function of the resolution k_{max} . This is shown on the right panel of Figure 4, at our resolution $k_{\text{max}} \sim 3000$, the accuracy of Equation 9 is better than 5%.

3 THE 2D GALAXY FIELD COVARIANCE MATRIX

As the galaxy power spectrum is among the most widely used statistic to extract information about cosmological parameters in large scale structures surveys, it is worth

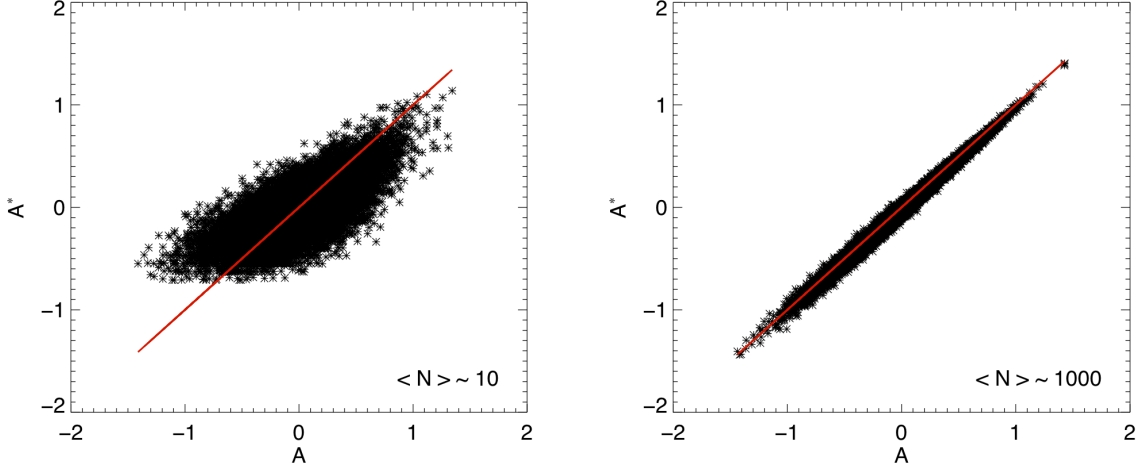


Figure 2. Scatter plot of A^* as a function of A for two different values of \bar{N} using $n_{cells} = 128^2$. The red lines represent the cell values for which $A^* = A$. When the survey is dense, i.e. when \bar{N} is large (right panel), there is almost no bias between A and A^* . However, for low density survey (left panel), A^* tends to be smaller than A leading to a bias between the two quantities.

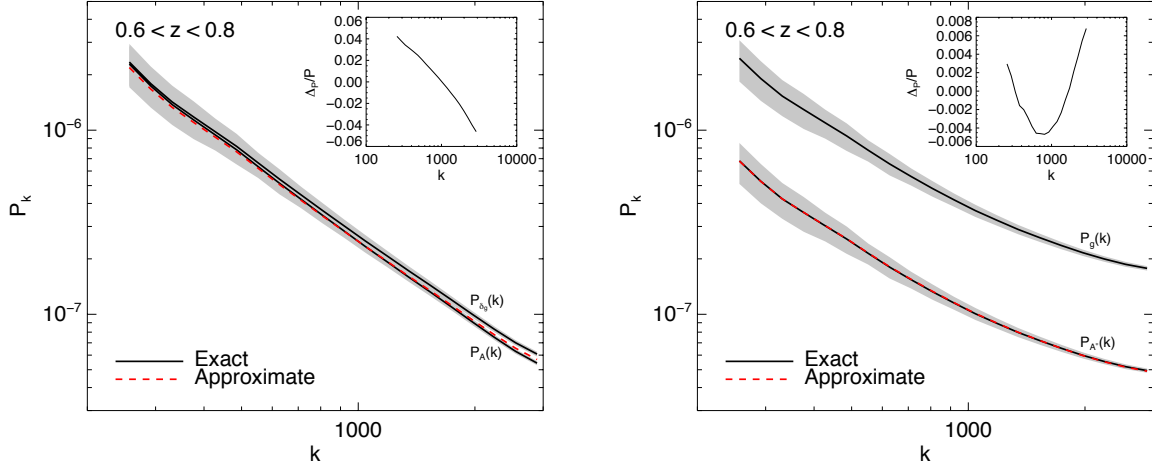


Figure 3. On the left panel, the solid black lines represent the prediction of power spectra of the underlying fields δ and $A = \ln(1 + \delta)$ in the redshift bin $0.6 < z < 0.8$. The dashed red line is the result obtained using Equation 3. On the right panel, predictions of both the galaxy angular power spectrum $P_g(k)$ and the non-linear transform A^* power spectrum $P_{A^*}(k)$ in the redshift bin $0.6 < z < 0.8$. The dashed red line is the result obtained using Equation 6. On both panels, the grey area shows the 1σ confidence regions and the inside panels show the deviation from the true value using our model.

quantifying how much information one can expect on a given parameter as a function of the survey characteristics and compare it to the total information on this parameter available from the data set.

Carron et al. (2014b) developed a useful, approximate form of the matter power spectrum in the mildly non-linear regime based on previous studies from N -body simulations (Neyrinck 2011; Mohammed & Seljak 2014):

$$\begin{aligned} \text{Cov}_{ij} &= \langle \hat{P}(k_i) \hat{P}(k_j) \rangle - \langle \hat{P}(k_i) \rangle \langle \hat{P}(k_j) \rangle \\ &= \delta_{ij} \frac{2 \left(P(k_i) + \frac{1}{\bar{n}} \right)^2}{N_{k_i}} + \sigma_{min}^2 P(k_i) P(k_j). \end{aligned} \quad (11)$$

The first term corresponds to the Gaussian covariance and the second term approximates the shell-averaged trispectrum of the field. It turns out that the parameter σ_{min}^2 can be interpreted as the minimum variance achievable on an amplitude-like parameter (see Carron et al. 2014b, for details). It can be further decomposed into two contributions:

$$\sigma_{min}^2 = \sigma_{SS}^2 + \sigma_{IS}^2. \quad (12)$$

The first term is due to the correlation between large wavelength “super-survey” modes with the small scales while the second term corresponds to the coupling between small scales or “intra-survey” modes.

Here we study local density fluctuations, $\delta = \frac{\rho - \bar{\rho}}{\bar{\rho}}$, defined with respect to the local observed density. In the par-

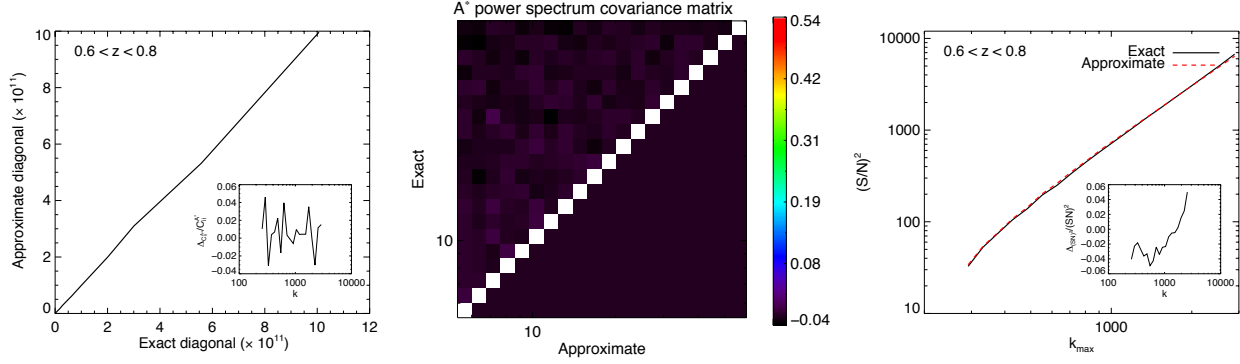


Figure 4. On the left panel, the diagonal of the A^* -power spectrum covariance matrix obtained using Equation 9 as a function of the exact value obtained with simulations. The middle panel represents the comparison between the approximate (lower right) and the exact (upper left) values of the normalised A^* -covariance matrix. At $< 10\%$ level, the analytical formula reproduces very well the exact prediction. The right panel shows the squared cumulative signal-to-noise for A^* obtained using approximation of Equation 9 compared to the exact value. At our resolution, the accuracy is better than 5%.

ticular case of a lognormal underlying distribution, there is a cancellation between two contributions in the covariance matrix resulting in $\sigma_{SS}^2 = 0$ (see Carron et al. 2014b, for details). Thus in our study, the only significant contribution comes from the “intra-survey” modes. We model σ_{min}^2 within the hierarchical *Ansatz* (Peebles 1980; Fry 1984; Bernardeau 1996), reducing to (see details in Carron et al. 2014b):

$$\begin{aligned} \sigma_{min}^2 &= \sigma_{IS}^2 = (4R_a + 4R_b) \frac{1}{\sigma_{\delta_g}^2} \frac{1}{V} \int \frac{dk}{2\pi} k P^2(k) \\ &\simeq \frac{P(k_{max})}{V} (4R_a + 4R_b) \end{aligned} \quad (13)$$

which decreases as the resolution increases.

Although it has been proved to be a good model in the 3-dimensional case, this approximation does not work particularly well in our case mostly for the fact that i) there are projection effects as we consider 2-dimensional clustering, ii) we probe here more non-linear scales ($k_{max} \sim 3000$). In fact this form of the covariance matrix is known to work until $k^{3D} < 0.8 \text{ hMpc}^{-1}$ while in our case $k_{max}^{3D} \sim 7 \text{ hMpc}^{-1}$ for $\bar{z} = 0.7$. Thus we propose a generalization introducing a scale dependent $\sigma_{min} = \sigma_{min}(k)$. Then *Ansatz* for the covariance matrix becomes:

$$\text{Cov}_{ij} = \delta_{ij} \frac{2(P(k_i) + \frac{1}{n})^2}{N_{k_i}} + \sigma_{min}(k_i) \sigma_{min}(k_j) P(k_i) P(k_j). \quad (14)$$

In order to estimate of $\sigma_{min}(k)$, we proceed as follows. The leading term of the trispectrum of the lognormal field is given by (see e.g. Takahashi et al. 2014) :

$$\begin{aligned} T(\mathbf{k}_i, -\mathbf{k}_i, \mathbf{k}_j, -\mathbf{k}_j) &= 2P(\mathbf{k}_i)P(\mathbf{k}_j)(P(\mathbf{k}_i) + P(\mathbf{k}_j)) \\ &+ (P(\mathbf{k}_i) + P(\mathbf{k}_j))^2 [P(|\mathbf{k}_i + \mathbf{k}_j|) + P(|\mathbf{k}_i - \mathbf{k}_j|)]. \end{aligned} \quad (15)$$

To obtain the spectrum covariance matrix, we need to average this expression, summing over all Fourier modes \mathbf{k}_i and \mathbf{k}_j in the corresponding bins of shells of the spectrum estimator. Assuming the bin width is small enough, this averaging affects only the term in square brackets. In the limit of a large number of modes and infinitesimal bin width, it is the average with respect to the angle θ between $\hat{\mathbf{k}}_i$ and $\hat{\mathbf{k}}_j$.

Table 1. Best-fitting slope n values and $\chi^2/\text{d.o.f}$ derived using the fitting formula $P(k) = A_s k^n$ on the 2-dimensional field predictions in the four redshift bins.

Redshift bin	n	$\chi^2/\text{d.o.f}$
$0.2 < z < 0.4$	-1.34	0.04
$0.4 < z < 0.6$	-1.38	0.07
$0.6 < z < 0.8$	-1.44	0.21
$0.8 < z < 1.0$	-1.63	0.21

On the diagonal ($k_i = k_j = k$) it takes the form

$$\frac{1}{2\pi} \int_{-\pi}^{\pi} P(k\sqrt{2+2\cos\theta}) d\theta. \quad (16)$$

It appears that for the relevant case of pure power law spectra $P \propto A_s k^n$ with realistic exponent, this integral diverges. We can correct this by separating the (in the real world finite and negligible) contribution of the background mode fluctuation $P(0)$ from the rest, which we still treat in the continuous limit. I.e. we write

$$\frac{1}{2\pi} \int_{-\pi+\epsilon}^{\pi-\epsilon} A_s (2k^2(1+\cos(\theta)))^{n/2} d\theta. \quad (17)$$

The cutoff parameter $\epsilon = \arctan(1/n_i)$, where $n_i = k_i L/(2\pi)$ is such that the integral starts at the first non-zero mode of the discrete Fourier modes associated to the grid. The integration gives:

$$\frac{2^{n+1}}{2\pi} P(k) B_{\cos^2(\epsilon/2)}(1/2, (n+1)/2) \quad (18)$$

where B is the incomplete beta-function. According to Equation 15, we have on the diagonal of the covariance of the galaxy field matrix:

$$\begin{aligned} \sigma_{min}^2(k_i) &= T_{ii}/P(k_i)^2 - \frac{2}{N_{k_i}} \\ &= 4P(k_i) \left[1 + \frac{2^{n+2} B_{\cos^2(\epsilon/2)}(1/2, (n+1)/2)}{2\pi} \right] \end{aligned} \quad (19)$$

To estimate the slope n , we adjust a power-law to the 2-dimensional power spectrum and use the best fit values presented in Table 1.

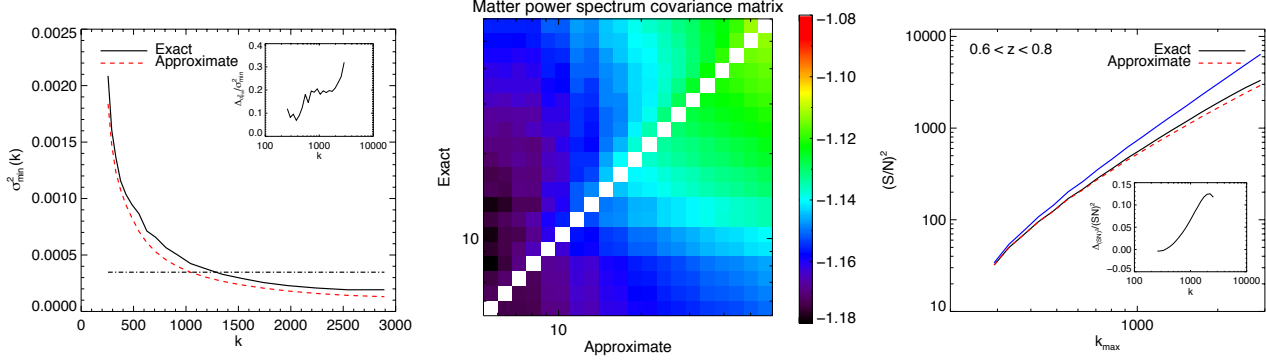


Figure 5. On the left panel, the comparison between the predicted value of $\sigma_{\min}^2(k)$ using the exact matter covariance matrix predicted by simulations compared to Equation 19 (red dashed line). As a comparison the dot-dashed line shows the value given by Equation 13 from Carron et al. (2014b). Our approximation reproduces well the shape of the true value within 30% at high- k and 10% at low- k . The middle panel shows the comparison between the exact (upper left corner) and the approximate (lower right corner) values of the matter covariance matrix. The right panel shows the squared cumulative signals-to-noise obtained using approximation of Equation 14 for the galaxy power spectrum covariance matrix compared to the exact value. At our resolution, the accuracy is within $\sim 10\%$.

The left panel of Figure 5 shows the comparison between the predicted value of $\sigma_{\min}^2(k)$ using the exact matter covariance matrix. The red dashed line shows $\sigma_{\min}^2(k)$ given by Equation 19 and as a comparison the dot-dashed line shows the value given by Equation 13. Our approximation reproduces well the shape of the true value within 30% at high- k and 10% at low- k . The middle panel of Figure 5 illustrates the comparison between the exact and the approximate covariance matrix while the right panel shows that the squared cumulative signals-to-noise agree within $\sim 10\%$.

4 INFORMATION CONTENT

We now have all the ingredients to quantify the Fisher information content of the A^* -power spectrum for cosmological parameters (which in the shot-noise free regime is very close to the total information). We can also compare the cosmological information content of the galaxy power spectrum to that of A^* . Our analytical model only requires on the prediction of the galaxy power spectrum P and of the shot-noise level of the considered survey through \bar{N} . Thus, for a given observation, we can forecast analytically the constraints on cosmological parameters extracted from the clustering of the underlying random field.

Given a set of parameters α, β, \dots , the Fisher matrix of the spectrum is defined as:

$$F_{\alpha\beta} = \sum_{k_i, k_j < k_{\text{max}}} \frac{\partial P(k_i)}{\partial \alpha} [\text{Cov}_{ij}]^{-1} \frac{\partial P(k_j)}{\partial \beta} \quad (20)$$

where the covariance matrix is given by Equation 14. The inverse of the Fisher matrix corresponds to the covariance of the posterior distribution of the parameters that could be obtained given the error bars one has on the data. It means that the larger the value of a Fisher matrix coefficient is, the smaller the variance becomes, and therefore, the tighter the constraint on the parameter.

The information content from A^* is given by:

$$F_{\alpha\beta}^{A^*} = \sum_{k_i, k_j < k_{\text{max}}} \frac{\partial P_{A^*}(k_i)}{\partial \alpha} [\text{Cov}_{ij}^{A^*}]^{-1} \frac{\partial P_{A^*}(k_j)}{\partial \beta}. \quad (21)$$

Thus Equation 6 leads to

$$\text{Cov}_{ij}^{A^*} = \frac{2b^4}{N_k} \left(P(k_i) + \frac{1}{\bar{n}} \right) \left(P(k_j) + \frac{1}{\bar{n}} \right) \delta_{ij}. \quad (22)$$

Equation 21 then becomes:

$$F_{\alpha\beta}^{A^*} = \frac{1}{2} \sum_{k < k_{\text{max}}} \frac{\partial \ln P_{A^*}}{\partial \alpha} N_k \frac{\partial \ln P_{A^*}}{\partial \beta} \quad (23)$$

with

$$\begin{aligned} \frac{\partial \ln P_{A^*}(k)}{\partial \alpha} &= \frac{\partial \ln b^2}{\partial \alpha} + \frac{\partial \ln P_g(k)}{\partial \alpha} \\ &= \frac{\partial \ln b_A^2}{\partial \alpha} + \frac{\partial P(k)}{\partial \alpha} \frac{1}{P(k) + 1/\bar{n}}. \end{aligned} \quad (24)$$

The bias coming from the A^* mapping is fixed by the fiducial values of HOD and cosmology and thus does not carry a cosmological dependence.

Finally:

$$\begin{aligned} F_{\alpha\beta}^{A^*} &= F_{\alpha\beta}^G + \frac{\partial \ln b_A^2}{\partial \alpha} \frac{\partial \ln b_A^2}{\partial \beta} (S/N)_G^2 \\ &+ \frac{\partial \ln b_A^2}{\partial \alpha} F_{\beta, \ln A_z}^G + \frac{\partial \ln b_A^2}{\partial \beta} F_{\alpha, \ln A_z}^G \end{aligned} \quad (25)$$

where:

$$F_{\alpha\beta}^G = \int d \ln k w(k) \frac{\partial \ln P(k)}{\partial \alpha} \frac{\partial \ln P(k)}{\partial \beta}. \quad (26)$$

with

$$w(k) = \frac{V}{2} \frac{k^2}{2\pi} \left(\frac{\bar{n}P(k)}{\bar{n}P(k) + 1} \right)^2. \quad (27)$$

corresponding to the usual formula from Tegmark (1997). We have replaced the discrete sums with integrals using the fact that the number of modes N_k is approximately the surface of the shell used for the bin averaging divided by the

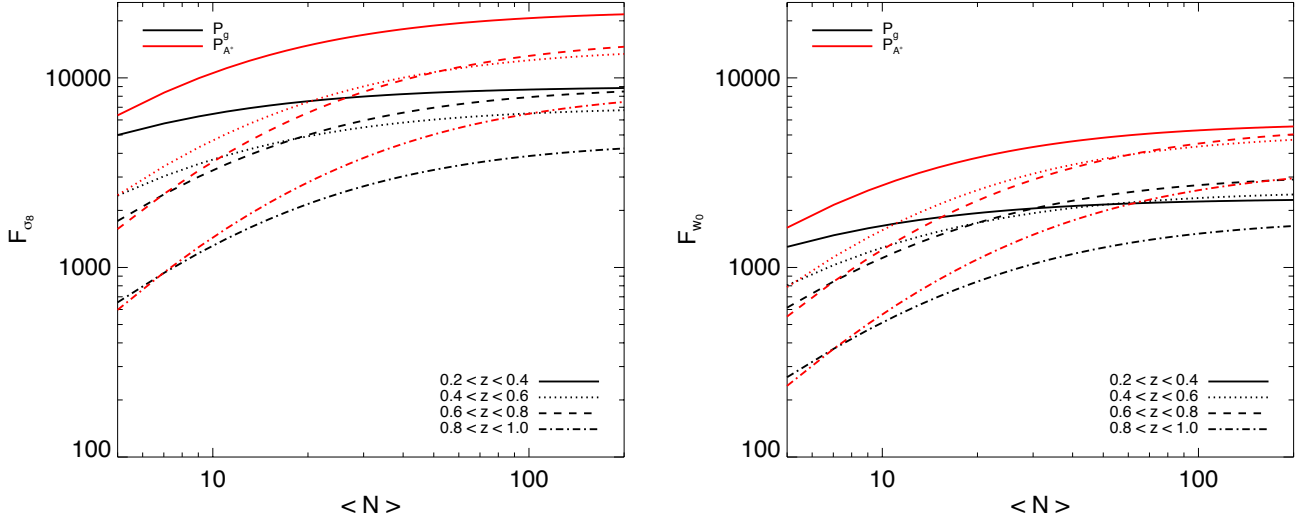


Figure 6. Fisher information of the A^* - (red lines) and galaxy power spectrum (black lines) as a function of the shot-noise level (through the sampling rate \bar{N}) for the two cosmological parameters σ_8 (left panel) and w (right panel) in the four redshift bins $0.2 < z < 0.4$, $0.4 < z < 0.6$, $0.6 < z < 0.8$ and $0.8 < z < 1.0$. For $\bar{N} > 5 - 7$, we see that the non-linear transform A^* performs better than the galaxy power spectrum over the whole range of number densities and redshifts to extract information on cosmological parameters. It can also be seen that the A^* -power spectrum is more powerful at low redshifts where the non-linearities are stronger, but also for dense survey (i.e for large values of \bar{N}).

distance element between two discrete modes. With our convention:

$$N_k \simeq V \frac{2\pi k dk}{(2\pi)^2} \quad (28)$$

Moreover, in Equation 25, by analogy to Carron et al. (2014b), we have introduced a nonlinear amplitude parameter $\ln A_z$ defined such as $\partial_{\ln A_z} P(k) = P(k)$. This parameter corresponds to the initial amplitude σ_8^2 in the linear regime and at $z = 0$. We further define the Gaussian signal to noise as:

$$(S/N)_G^2 = \int d\ln k \frac{V}{2} \frac{k^2}{2\pi}. \quad (29)$$

corresponding to a case without shot-noise. The derivatives are estimated numerically using the **CosmoPMC** package.

The panels of Figure 6 show the A^* - and galaxy power spectrum Fisher information as a function of \bar{N} for the two cosmological parameters σ_8 (left panel) and w (right panel) in the four redshift bins $0.2 < z < 0.4$, $0.4 < z < 0.6$, $0.6 < z < 0.8$ and $0.8 < z < 1.0$. We consider values of $\bar{N} > 5$ where A^* is expected to start to perform better. We can clearly see that for small \bar{N} , the shot-noise erases information present in the underlying random field. As previously seen in Wolk et al. (2014), the analytical approach developed in this work reproduces well the general trends expected for the non linear transform A^* : i) for $\bar{N} > 5 - 7$, A^* performs better than the galaxy power spectrum over the whole range of number densities and redshifts and thus could be used to unveil the otherwise hidden information, ii) the use of the A^* -power spectrum to extract the information is more powerful at low redshifts where the non-linearities are stronger, and iii) our observable is more efficient for dense survey (i.e for large values of \bar{N}).

To compare in a quantitative way our results with the previous forecasts of Wolk et al. (2014), Figure 7 shows the predicted improvement in the information on w_0 (left panel) and σ_8 (right panel) as a function of redshift and the survey shot-noise level. The quantity plotted is the ratio between the galaxy and A^* -power spectrum Fisher matrix elements. In that sense, it represents the expected information gain using the non-linear transform A^* instead of the power spectrum. The simplest interpretation of this gain is an effective gain in survey area. We also show for illustrative purposes, the values of \bar{N} for different upcoming surveys in the first redshift bin where the gain is known to be the highest (see Wolk et al. 2014, for details).

This analytical approach reproduces better than 20% the expected gain for the two parameters σ_8 and w_0 . Qualitatively, the achievable gain is about a factor of 2, especially at low redshifts and for dense surveys. We conclude that the analytical model developed here using the matter power spectrum at a redshift z and the number density of the survey, is able to predict the constraints on cosmological parameters from galaxy clustering with reasonable precision.

5 DISCUSSION

It has been known that non-linear transforms help to capture more efficiently the information encoded in the matter density field. The notion of *sufficient statistics* (Carron & Szapudi 2013) has emerged as the optimal transformation that extracts all cosmological information. In the case of a discrete galaxy field the new observable A^* was constructed (Carron & Szapudi 2014). Wolk et al. (2014) have forecasted using a numerical approach the expected improvement on constraints beyond that of using the galaxy power spectrum

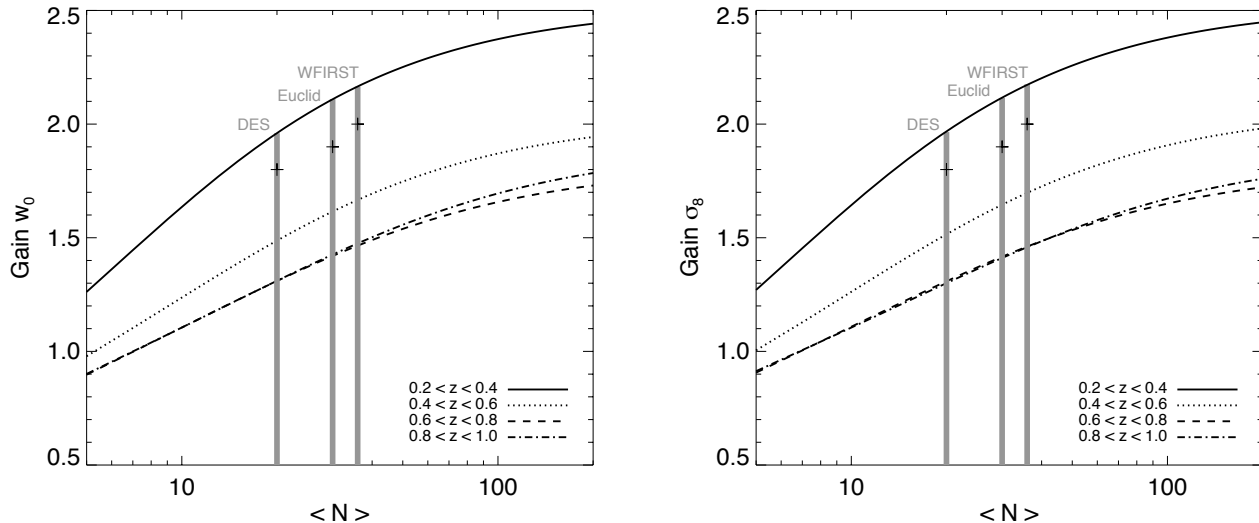


Figure 7. Information gains on the cosmological parameters w_0 (left panel) and σ_8 (right panel) using the A^* power spectrum instead of the galaxy power spectrum as a function of the shot-noise level in the survey (through the sampling rate \bar{N}). We recover the gain predicted numerically in Wolk et al. (2014) (black crosses) which was about a factor of 2, especially at low redshifts and for dense surveys. Illustrated by the vertical lines, the values of \bar{N} for different upcoming surveys in the first redshift bin $0.2 < z < 0.4$.

on the latest CFHTLS data set as well as on upcoming large wide-field surveys; for the former, the forecast agreed well with the actual gain realized when calculating the A^* power spectrum. In this work, we have developed an analytical approach that captures the statistics of A^* to the point that we could accurately forecast the best achievable constraints on cosmological parameters as a function of the survey density. The forecast improvement is consistent with previous, more tedious, numerical calculations at the 20% level at worst (or 10% for error bars).

We have presented an Ansatz for the bias between the galaxy and A^* -power spectra, and demonstrated its accuracy compared to the previous numerical approach. We showed that the dependence of the bias on cosmology is crucial for endowing A^* with the ability to recapture the hidden information from the field. In addition, we proposed a diagonal form for the A^* power spectrum covariance matrix and showed that it is accurate at the 5% level.

In order to compare with the standard method of extracting cosmological parameters from the galaxy power spectrum, we have provided and explored the accuracy of an analytical Ansatz for the projected power spectrum covariance matrix. Based on a generalization of Carron et al. (2014b), we were able to reproduce squared cumulative signals-to-noise of the matter field within 10%.

Although our analytical framework contains a fair number of approximations, we have demonstrated that our forecasts are reliable at least within 20% even at the most non-linear scales we probed. Moreover, our method includes all the non-Gaussian effects (super survey modes, trispectrum, discreteness) and thus it is expected to be more accurate than the standard Gaussian forecasts entirely ignoring such effects. In addition, the approach has also provided new

insights and a deeper understanding of the cosmological information content of the galaxy clustering.

Finally, we predicted the best achievable constraints on the cosmological parameters: σ_8 and w_0 as a function of the shot-noise level in the survey. We were able to recover, the predictions from Wolk et al. (2014) using a large ensemble of numerical simulations, and found that the gain on the information using the A^* -power spectrum translates into factor of 2 gain approximately, especially at low redshifts and for dense surveys.

The promise of A^* for improving cosmological constraints from future surveys has been clear for a while. However, until now, the prediction of its power spectrum involved a large number of numerical simulations, a disadvantage when used in an MCMC sampling framework to fit cosmological parameters. Likewise, the corresponding covariance matrices also needed massive number of simulations. The present work provides a convenient and accurate short cut, that can be used at least for forecasting purposes, and it has the potential of speeding up MCMC sampling as well. The present approximations have been tested for 2-dimensional projected surveys, but similar developments can be carried out for 3-dimensional surveys as well. Previous attempts have been made using dark matter simulations, however, it is worth mentioning that the information gain is volume dependent and changes with respect to a local or global description (i.e if we consider density fluctuations defined with respect to the local observed density or not, see Carron et al. 2014b). Neyrinck et al. (2009) using the local density field from the $500 \text{ h}^{-1} \text{ Mpc}$ Millenium simulation (Springel 2005) found a factor of ~ 10 improvement on the information on the $(S/N)^2$ (corresponding approximately to $\ln(\sigma_8^2)$ unmarginalized over the other cosmological parameters) using sufficient statistics. Neyrinck (2011)

doing the same analysis on the Coyote Universe (Heitmann et al. 2009, 2010) which have a box size of 1300 Mpc, found then an improvement of ~ 15 . More recently, Wolk et al. (2015) considering the constraints on neutrino mass from the DEMNUNI simulation of volume $V = 8 \text{ h}^{-3} \text{ Gpc}^3$ using both the power spectrum and sufficient statistics found a factor ~ 8 improvement on the information. A similar framework to the present for 3-dimensional surveys including the effects of redshift space distortions both on the power spectra and on covariance matrices would be desirable for applications, and are left for future work.

The authors acknowledge NASA grants NNX12AF83G and NNX10AD53G for support.

Part of this work was based on observations obtained with MegaPrime/MegaCam, a joint project of CFHT and CEA/IRFU, at the Canada-France-Hawaii Telescope (CFHT) which is operated by the National Research Council (NRC) of Canada, the Institut National des Science de l'Univers of the Centre National de la Recherche Scientifique (CNRS) of France, and the University of Hawaii. This work is based in part on data products produced at Terapix available at the Canadian Astronomy Data Centre as part of the Canada-France-Hawaii Telescope Legacy Survey, a collaborative project of NRC and CNRS.

REFERENCES

- Bernardeau F., 1996, *A&A*, 312, 11
 Carron J., Neyrinck M. C., 2012, *ApJ*, 750, 28
 Carron J., Szapudi I., 2013, *MNRAS*, 434, 2961
 Carron J., Szapudi I., 2014, *MNRAS*, 439, L11
 Carron J., Wolk M., Szapudi I., 2014a, *MNRAS*, 444, 994
 Carron J., Wolk M., Szapudi I., 2014b, *ArXiv e-prints*
 Fry J. N., 1984, *ApJ*, 279, 499
 Heitmann K., Higdon D., White M., Habib S., Williams B. J., Lawrence E., Wagner C., 2009, *ApJ*, 705, 156
 Heitmann K., White M., Wagner C., Habib S., Higdon D., 2010, *ApJ*, 715, 104
 Joachimi B., Taylor A. N., 2011, *MNRAS*, 416, 1010
 Lewis A., Challinor A., Lasenby A., 2000, *Astrophys. J.*, 538, 473
 Mohammed I., Seljak U., 2014, *MNRAS*, 445, 3382
 Neyrinck M. C., 2011, *ApJ*, 736, 8
 Neyrinck M. C., Szapudi I., Rimes C. D., 2006, *MNRAS*, 370, L66
 Neyrinck M. C., Szapudi I., Szalay A. S., 2009, *ApJ*, 698, L90
 Peebles P. J. E., 1980, *The large-scale structure of the universe*
 Rimes C. D., Hamilton A. J. S., 2005, *MNRAS*, 360, L82
 Seo H.-J., Sato M., Dodelson S., Jain B., Takada M., 2011, *ApJ*, 729, L11
 Springel V., 2005, *MNRAS*, 364, 1105
 Szapudi I., 2009, in Martínez V. J., Saar E., Martínez-González E., Pons-Bordería M.-J., eds, *Lecture Notes in Physics*, Berlin Springer Verlag Vol. 665, *Data Analysis in Cosmology*. pp 457–492
 Takahashi R., Soma S., Takada M., Kayo I., 2014, *MNRAS*, 444, 3473
 Tegmark M., 1997, *Physical Review Letters*, 79, 3806
 Wolk M., Carron J., Szapudi I., 2014, *ArXiv e-prints*
 Wolk M., Szapudi I., Bel J., Carbone C., Carron J., 2015, in prep.